

J. Ongena, Yu. Baranov, V. Bobkov, C.D. Challis, S. Conroy, A. Ekedahl, G. Ericsson, M. Goniche, Ph. Jacquet, I. Jenkins, L. Giacomelli, C. Hellesen, A. Hjalmarsson, J. Källne, V. Kiptily, K. Kirov, A. Krasilnikov, M. Laxåback, E. Lerche, J. Mailloux, M.L. Mayoral, I. Monakhov, M. Nave, V. Petrzilka, K. Rantamaki, E. Solano, D. Van Eester, A. Walden and JET EFDA contributors

Heating Optimization Studies at JET in Support of ITER

"This document is intended for publication in the open literature. It is made available on the understanding that it may not be further circulated and extracts or references may not be published prior to publication of the original when applicable, or without the consent of the Publications Officer, EFDA, Culham Science Centre, Abingdon, Oxon, OX14 3DB, UK."

"Enquiries about Copyright and reproduction should be addressed to the Publications Officer, EFDA, Culham Science Centre, Abingdon, Oxon, OX14 3DB, UK."

Heating Optimization Studies at JET in Support of ITER

J. Ongena¹, Yu. Baranov², V. Bobkov³, C.D. Challis², S. Conroy⁴, A. Ekedahl⁵,
G. Ericsson⁴, M. Goniche⁵, Ph. Jacquet², I. Jenkins², L. Giacomelli⁴, C. Hellesen⁴,
A. Hjalmarsson⁴, J. Källne⁶, V. Kiptily², K. Kirov², A. Krasilnikov⁷, M. Laxåback⁸,
E. Lerche¹, J. Mailloux², M.L. Mayoral², I. Monakhov², M. Nave⁹, V. Petrzilka¹⁰,
K. Rantamaki¹¹, E. Solano¹², D. Van Eester¹, A. Walden² and JET EFDA contributors

JET-EFDA, Culham Science Centre, OX14 3DB, Abingdon, UK

¹Association “EURATOM - Belgian State” Laboratory for Plasma Physics Koninklijke Militaire School -
Ecole Royale Militaire, Brussels, Belgium, TEC Partner

²EURATOM-UKAEA Fusion Association, Culham Science Centre, OX14 3DB, Abingdon, OXON, UK

³Max Planck IPP-EURATOM Assoziation, Garching, Germany

⁴Association EURATOM-VR, Department of Physics and Astronomy, Uppsala University, Uppsala, Sweden

⁵Association EURATOM-CEA, CEA/Cadarache, France

⁶Association EURATOM-VR, Department of Engineering Sciences, Uppsala University, Uppsala, Sweden

⁷SRC RF Troitsk Institute for Innovating and Fusion Research, Troitsk, Russia

⁸Association EURATOM-VR, Fusion Plasma Physics, EES, KTH, Stockholm, Sweden

⁹Associação EURATOM/IST, Centro de Fusão Nuclear, Instituto Superior Técnico, Lisbon, Portugal

¹⁰Association EURATOM-IPP.CR, Institute of Plasma Physics AS CR, Praha, Czech Republic

¹¹VTT Technical Research Centre of Finland, Association EURATOM-Tekes, Finland

¹²Association EURATOM-CIEMAT, Madrid, Spain

* See annex of F. Romanelli et al, “Overview of JET Results”,
(Proc. 22nd IAEA Fusion Energy Conference, Geneva, Switzerland (2008)).

Preprint of Paper to be submitted for publication in Proceedings of the
22nd IAEA Fusion Energy Conference, Geneva, Switzerland.

(13th October 2008 - 18th October 2008)

ABSTRACT.

Experiments have been performed at JET in view of optimizing the heating systems for ITER. To optimize coupling of ICRH in ITER with foreseen large antenna-plasma distances, gas puffing in the SOL has been successfully applied. Up to 8MW of ICRF power has been coupled in this way to ELMy H-Mode plasmas. The D fundamental ICRH heating scheme was further explored in combined ICRH and deuterium NBI heated deuterium discharges in JET. A concentration of fast deuterons less than 10% is able to absorb up to half of the ICRH power, rendering the fundamental D heating scheme much more viable for ITER. A possible caveat is that due to the large Doppler shift of 1MeV beam ions in ITER, absorption of ICRH waves could also occur in scenarios where the cold resonance layer is outside of the plasma. Anomalous behaviour of the beam ions has been observed at high densities (close to the Greenwald limit). The effects cannot be explained by the MHD effects or sawteeth, and an anomalous diffusion coefficient has to be assumed for passing fast particles with pitch angles $v_{\parallel}/v > 0.7$. This result has possible implications for beam heating on ITER.

1. COUPLING OF ICRH POWER AT LARGE ANTENNA-PLASMA DISTANCES

Coupling of 20MW of Ion Cyclotron Resonance Frequency (ICRF) power in H-mode plasmas using one ITER port [1] will be a challenging task. Over the past few years, however, significant progress towards this goal is made [2] but the coupling of the RF waves at large distances between antenna and plasma separatrix and/or in ELMy H-Mode plasmas is still challenging. The difficulty is twofold: (i) the large distance between the antenna Faraday screen and the plasma separatrix distance (up to 14cm) leads to a reduction in the ICRF power reaching the plasma due to the exponential decrease of the antenna loading with increasing distance to the fast wave cut-off density [3-4]; (ii) the presence of Edge Localised Modes (ELMs) in H-mode plasmas results in very fast changes in loading for ICRF antennae. Several solutions are envisaged to couple steady ICRF power during such changes [5-9]. However, studying loading perturbations during ELMs requires fast acquisition systems and was until now only scarcely documented [10-12], in particular for large distances between plasma and antenna.

For the first time in JET, experiments were performed with both challenges combined [13].

The variation in the loading of the JET A2 antennae [14] was monitored with a fast data acquisition system (with sampling rates up to 4 μ s). Based on earlier studies on the influence of the Scrape-Off-Layer (SOL) on the coupling of ICRF and LH antennae [15-16], injection of deuterium (D_2) gas in the edge was tried in order to bring the fast wave cut-off layer closer to the antenna. High triangularity ($\delta \sim 0.4$) H-mode plasmas with low amplitude/high frequency type I ELMs were used. In order to cover ITER-relevant distances, the Radial Outer Gap (ROG), defined as the distance in the midplane between separatrix and poloidal limiters, was varied between 8 and 14cm. Hydrogen minority heating at 47MHz with “dipole” antenna phasing was applied. Apart from the expected variations in the coupling resistance during ELMs, a clear decrease in the perturbations caused by the ELMs on the coupling resistance was observed with increasing ROG. Furthermore, a decrease of the

baseline coupling (value of the coupling resistance in between ELMs) is seen when gas injection was stopped. Details of the effect of the D_2 gas injection are shown in Fig. 1, where the variation of the baseline value of coupling resistance of strap 4 of antenna B, $R_c(B4)$, is shown as a function of ROG and for various combinations of Gas Inlet Modules (GIM). The main observations are: (i) the coupling resistance without gas injection (triangles) is very low ($\sim 0.5\Omega$) and does vary only slightly for ROG values between 10 and 14 cm (as expected); (ii) the location of the gas injection plays an important role: with GIM 6 (located in the midplane) much less gas has to be used for a given increase in coupling resistance (see Pulse No: 68809 and 68110) than with the ringlike divertor GIMs 9 and 10. Combined use of GIM 9, 10 and 6 (total gas injection rate of $1.8 \cdot 10^{22}$ el/s, Pulse No: 68110), allowed to couple more than 8MW of ICRF power at a ROG of 14cm in ELMy H-mode plasmas in JET. A clear increase in the central electron temperature and plasma diamagnetic energy was observed, confirming a good absorption of the ICRF waves (see Fig.3). Further tests were done in order to investigate the possible influence of a magnetic connection between the location of the GIMs and the location of the antennae. D_2 gas was injected from GIM6 (located in the midplane) magnetically connected to antenna B, GIM2 (located in the midplane) magnetically connected to antenna A and GIM 8 (located at the top) magnetically connected to antenna B. None of these gas inlets was magnetically connected to antenna C. The change in baseline coupling for antenna A, B and C as a function of the gas injection rate from the different GIMs is shown in Fig. 3. Interestingly, improvement on all three antennas independent of the location of the GIM was observed; in particular an improvement was observed even if there was no magnetic connection between antenna and GIM. This suggests that D_2 injection both from the midplane and from the top leads to an increase in the SOL density throughout the whole equatorial plane. On the other hand, however, the improvement in coupling resistance for antenna A was noticeably higher using GIM2 and GIM8 compared to GIM6. These preliminary tests show that by carefully choosing the position of the gas inlet, one should be able to minimize detrimental effects on plasma confinement and at the same time efficiently increase the coupling resistance. However, a better understanding is needed on the influence of the position of the gas inlet, for ionizing the gas and modifying the SOL and for fuelling the plasma. Further JET experiments in this direction are planned as well the development of 3D edge modelling tools.

2. FUNDAMENTAL D HEATING EXPERIMENTS IN JET

Experiments were carried out in the JET tokamak in plasmas with 90-95% D (including thermal and NBI deuterons) to investigate the fundamental Deuterium majority ICRH scheme [17]. At typically $B_0 = 3.3T$, this implied $f = 25MHz$ to position the D ion-cyclotron layer near the plasma centre ($R_0 \approx 3m$).

At this frequency the ICRH power available on JET is strongly limited. Unlike previous experiments [18], in which the D concentration was much smaller than 90%, mode conversion was practically absent and the fraction of the ICRH power absorbed by the electrons is mainly associated

with Fast Wave Landau Damping (FWLD) and/or Transit-Time Magnetic Pumping (TTMP). Up to ~2MW of ICRF power was coupled to the plasma, leading to an increase in both electron and ion temperatures of approximately $\Delta T_e \approx 0.7\text{keV}$ and $\Delta T_i \approx 1.5\text{keV}$. The net result was that by adding ~25% of ICRH heating power to the discharge ($P_{\text{ICRH}} = 1.7\text{MW} / P_{\text{NBI+OH}} = 7\text{MW}$) the DD fusion power was increased by 30-50%, depending on the details of the experiment. The total neutron rate, the diamagnetic energy and the central electron and ion temperatures scaled linearly with the applied RF power in the studied range [17]. The neutron yield measured during the combined NBI+ICRF phases of the experiments exceeds the sum of the individual counts obtained in the RF-only and the NBI-only phases, pointing to a synergy between NBI and ICRH. This is likely to result from the fact that the beam injected fast deuterons, because of their larger Doppler-shifts, absorb the ICRF power more efficiently than the thermal deuterons, which suffer from the characteristic adverse polarization of the RF electric fields near the cold cyclotron resonance layer of the majority ions [19]. The RF absorption of the NBI ions causes an increase in their slowing down time leading to an enhancement in the DD reactions and therefore higher neutron yield.

This is consistent with the observed modification of the slowing down time estimated from the changes in the electron temperature and density in the presence of ICRH. The synergy between ICRH and NBI is further supported by neutron yield measurements performed with the fast neutron camera diagnostic [20], by fast particle measurements done with the neutral particle analyzer [21] and by the time-of-flight neutron spectro-meter TOFOR [22-23].

For the D majority ICRH experiments in JET, the Doppler-shifted ICRF beam absorption was investigated in detail by means of a coupled full-wave/QLFP numerical package [19], and was confirmed by the determination of the experimental power absorption profiles of the ions, estimated using an improved break-in-slope analysis [24] based on Charge eXchange Recombination Spectroscopy (CXRS) available at JET [25]. The results of the full-wave module have shown that the beam deuterons absorb nearly half of the RF power injected in the plasma, even at the modest concentrations (~6-8%) characteristic for the experiments (see Fig.4).

The QLFP simulations indicated that, at the modest ICRH power available in the experiments ($P_{\text{RF}} \leq 2\text{MW}$), the RF-induced energy tail of the beam particles is restricted to $E < 200\text{keV}$. On the other hand, a considerable increase in the ‘slowing-down’ population of the beam ions (with energies between 20-130keV) was obtained in the simulations. This effect is particularly dominant in the inner magnetic surfaces, where the beam ions with higher energies (around 130keV) are not resonant while the slowing-down beam ions (with lower energies) still are. These results are in good agreement with the experimental observations: the neutron spectrometer TOFOR (with vertical line-of-sight close to the plasma centre) detected a substantial increase in the population of slowing-down beam ions when ICRH power is applied on top of NBI (Fig.5a) while the creation of a modest RF heated tail was observed by NPA (with horizontal line-of-sight) in the energy range 120-200keV (Fig.5b). Since the number of deuterons detected above the NBI injection energy is small, it is believed that the increased population of slowing-down deuterons is mainly responsible for the enhanced neutron

yield observed during the combined NBI+ICRH phases of the experiments. The interaction of fast NBI ions with ICRF was already addressed earlier [26,27] and has been noticed in past DIII-D [28] and JET [29] experiments. In recent 3He-D mode conversion experiments at JET [30], a clear separation was expected between direct electron heating from mode conversion and ion heating from ^3He minority heating, because due to its 3 times heavier mass, minority heating of 3He in (^3He)-D plasmas produces less energetic tails than those observed in (H)-D experiments, and thus these mode-ately energetic ^3He tails predominantly slow down on ions. Unexpectedly, strong ICRF induced D-tail formation was observed in those discharges. A tail of D-ions was clearly detected by gamma ray spectroscopy, as a distinct peak at 3.09MeV was observed from the reaction $^{12}\text{C}(d,p\gamma)^{13}\text{C}$ at high ^3He concentrations ($X[^3\text{He}] = n^3\text{He}/n_e > 20\%$) while it is totally absent at low concentrations ($X[^3\text{He}] \sim 10\%$, in ^3He minority heating experiments). Neutron time-of-flight spectra from the TOFOR neutron spectrometer [22, 23] are shown in Fig.6 for JET Pulse No's: 69388 (left), 69392 (middle) and 69393 (right). For Pulse No: 69388, $X[^3\text{He}] = 10\text{-}12\%$ (minority ion heating regime) while for 69393 it was $X[^3\text{He}] = 18\%$ (mode conversion electron heating regime); Pulse No: 69392 is similar to Pulse No: 69393 except that the NBI power was 8MW (all by 130keV injectors), while that of 69393 was 16MW. All 3 shots were done at 33MHz and with similar RF power ($\sim 4\text{-}4.5\text{MW}$). The neutron time-of-flight spectra are dominated by a peak around 65ns, which primarily corresponds to neutrons of 2.45MeV from $\text{D}+\text{D} \rightarrow ^3\text{He}+\text{n}$ fusion reactions involving the NBI ions and the thermal bulk plasma. Whereas the shape of the spectra for the main (65ns) peak are similar for Pulse No's: 69388 and 69393, a clear high-energy neutron tail is emerging as time progresses for Pulse No's: 69392 and 69393 while it is absent in the 69388 data. From a more detailed analysis of the TOFOR data it is seen that the high-energy neutron tail in the mode conversion regime Pulse No: 69393 corresponds to a high-energy deuterium tail whose temperature exceeds 300keV around $t = 9\text{s}$.

As for the majority D experiments, the combined use of RF and NBI heating is thought to be the key for understanding the D tail formation, as already suggested in [29] based on a resonance location analysis: with a thermal background, the deuterons hardly feel the presence of the RF fields since $\omega = \Omega_{\text{D}}$ is at $R = 2.4\text{m}$ i.e. about 0.6m away from the core ($\omega = \Omega_{^3\text{He}}$ is at $R = 3.21\text{m}$) and thus large RF power levels would be required to drive tails starting from thermal bulk D ions in this relatively cold region. Because JET is equipped with up to 130keV beams, the Doppler shifted resonance for NB injected D particles is however shifted up to 0.5m towards the core. At the time of the first mode conversion experiments, no sufficiently sophisticated wave + Fokker-Planck modelling tools were available to quantitatively substantiate the role of the Doppler shift and study the formation of non-Maxwellian tails self-consistently. The more recent modelling indicates that - when tuning the RF frequency and/or the magnetic field to ensure core ^3He heating - the RF absorption is maximal at minor radius $\rho \sim 0.4\text{m}$ i.e. both well away from the cold plasma resonance (at $\rho \sim 0.6\text{m}$) and the location at which the neutral beam particles are dominantly ionized (at $\rho \sim 0.2\text{m}$) [30].

3. ANOMALOUS DIFFUSION OF FAST BEAM IONS IN JET

The understanding of fast ion physics in tokamak plasmas is important for modelling and interpretation of neutral beam injection experiments. It is required for the derivation of transport coefficients and for the simulation of heating and current drive in beam heated plasmas and is thus important for extra-polation to ITER.

Various models exist to describe fast ion behaviour, however, such simulations do not always reproduce experimental effects. Trace Tritium Experiments (TTE) on JET were analysed using Monte Carlo modelling of the neutron emission resulting from the Neutral Beam Injection (NBI) of short (~300ms) Tritium (T) beam blips into reversed shear, hybrid ELMy H-mode and L-mode deuterium plasmas for a wide range of plasma parameters. The calculated neutron fluxes from Deuterium-Tritium (DT) reactions could only be made consistent with all plasmas by applying an artificial reduction of the T beam power in the modelling of between 20 and 40%. A similar discrepancy has previously been observed in both JET [31] and TFTR [32], although no mechanism has yet been found that could explain such a difference in the measured T beam power.

Applying this correction in the T beam power, good agreement between calculated and measured DT neutron emission profiles was obtained in low to moderate line averaged density ($\bar{n}_e < 4 \times 10^{19} \text{ m}^{-3}$) ELMy H-Mode plasmas assuming that the fast beam ions experience no, or relatively small, anomalous diffusion ($D_{\text{an}} < 0.5 \text{ m}^2/\text{s}$). Figure 8 shows that for the on-axis T blip during Pulse No: 61236 ($n_e(0) = 3.0 \times 10^{19} \text{ m}^{-3}$) the TRANSP [33] code satisfactorily matches the 14MeV neutron rate and neutron profile measured on the 2D neutron camera (Fig.7) with no anomalous diffusion if a reduction in T power of 20% is applied. Introducing a low level ($D_{\text{an}} = 0.5 \text{ m}^2/\text{s}$) of anomalous diffusion degrades the agreement in both 14MeV rate and profile. However, the modelled neutron profiles do not agree with measurements in higher density plasmas using the same assumption and the disagreement between the measured and calculated shape of the neutron profile increases with plasma density. Large anomalous losses of fast ions have to be assumed in the simulations to improve agreement between experimental and simulated neutron profiles, characterized by the goodness of fit. Pulse No: 61430 is the case with the highest density ($n_e(0) = 3.03 \times 10^{19} \text{ m}^{-3}$) and thus where the discrepancy is the most pronounced. Figure 9 shows the measured 14MeV neutron profile along with simulations for various types of fast ion loss varying from constant anomalous diffusion cases $D_{\text{an}}(r,t) = 0$ and $D_{\text{an}}(r,t) = 5 \text{ m}^2/\text{s}$ to cases simulating preferential losses of trapped particles (i.e. fast ions with a high ratio of perpendicular velocity to total velocity, $v_{\perp}/v > 0.75$) and preferential losses of passing particles (with $v_{\parallel}/v < 0.70$). Each of these cases was optimised in terms of the reduction in T power to achieve a minimum χ^2 when comparing the measured and simulated neutron profiles as shown in Table 1.

Though the case preferentially losing passing ions reproduces some aspects of the experimental profile, this is only a first approach and more sophisticated models will be required in order to gain a more detailed understanding of the nature of those losses. These results show that large anomalous losses should be introduced for specific groups of fast ions to reconcile measurement and simulation in high density plasmas.

CONCLUSIONS

ICRH and NBI experiments have been performed on JET in view of optimizing these systems for ITER. Optimization of the coupling of ICRH at large antenna-plasma distances has been obtained using D2 gas puffing. Two plasma configurations at high triangularity ($\delta \sim 0.4$) and different heating schemes were used to verify the applicability of this procedure under various conditions, and 8MW of ICRF power could be coupled at a ROG of 14cm (mean distance between antennastrap and plasma separatrix of ~ 19 cm) at a coupling resistance of 3-4 Ohm. The viability of D fundamental ICRH heating was further explored in combined ICRH and deuterium NBI heated deuterium discharges in JET. During NBI heating in those discharges, a strong increase of the neutron rate was observed, which is mainly attributed to the Doppler-shift in the ion-cyclotron resonance absorption of the fast beam ions. Combining results from the recently installed time-of-flight diagnostic TOFOR with new modeling tools has shown that the fast D beam injected particles (5-10% of the total population) are responsible for the absorption of 30-40% of the ICRH power, thus rendering a mechanism with normally poor absorption to a much more viable one for ITER. Another lesson learnt from this study is that in ITER, with foreseen 1 MeV beams and resulting large Doppler shift, absorption of ICRH waves could occur even if the D cyclotron layer is near the plasma boundary or even outside the plasma, as is e.g. the case for second harmonic T heating. Detailed analysis of experiments with short T blips has revealed anomalous behaviour of the beam ions at high densities (close to the Greenwald limit). The effects cannot be explained by the MHD effects or sawteeth, and an anomalous $D \sim 10 \text{ m}^2/\text{s}$ has to be assumed for passing fast particles with pitch angles $v_{\parallel}/v > 0.70$ to get agreement with experimental observations.

ACKNOWLEDGEMENTS

This work, supported by the European Communities under the contract of Association with EURATOM, was carried out within the framework of EFDA. The views and opinions expressed herein do not necessarily reflect those of the European Commission.”

REFERENCES

- [1]. ITER Physics Basis, Nucl. Fusion **39**, 2495-2539 (1999)
- [2]. Swain D. and Goulding R., Fusion Eng. and Design **82**,603-609 (2007)
- [3]. F. Clairet *et al.*, Plasma Phys. Cont. Fusion **46**, 1567-1580 (2004)
- [4]. Bilato R. et al., Nucl. Fusion **45**, L5-L7 (2005)
- [5]. Noterdaeme J.-M. et al., Fusion Eng. and Design **74** (2005) 191-198
- [6]. Vulliez K. et al., Nuclear Fusion, **48**, 065007 (2008)
- [7]. Mayoral M.L. et al., 17th Topical Conf. on Radio Frequency Power in Plasmas, Clearwater, AIP Conf. Proceedings **933**, 143-146 (2007)
- [8]. Monakhov I. et al., 15th RF Topical Conf. on Radio Frequency Power in Plasmas, Moran, AIP Conf. Proceedings **694**,150-153 (2003)

- [9]. Durodie F. et al., Fusion Eng. and Design **74**, 223 (2005)
- [10]. Pinsker R. et al., Proc. 31st EPS Conf. on Plasma Physics, London, UK, ECA, Vol. 28G, P2.175 (2004)
- [11]. Noterdaeme J.M. et al 1994 Proc. 21st EPS Conf. on Control Fusion and Plasma Phys. (1994, Montpellier, France) (ECA vol 18B Part II) pp. 842-845 (1994)
- [12]. Monakhov I. et al., 15th RF Topical Conference on Radio Frequency Power in Plasmas Moran, AIP Conf. Proceedings **694**, 146-149 (2003)
- [13]. Mayoral M.L., et al., 17th Topical Conf. on Radio Frequency Power in Plasmas, Clearwater, AIP conf. proceedings **933**, 55-58 (2007)
- [14]. Kaye A. et al, Fusion Eng. and Design **24**, 1-21 (1994)
- [15]. Parisot A. et al., Plasma Phys. Control. Fusion **46**, 1781-92 (2004)
- [16]. Ekedahl A. et al, Nucl. Fusion **45** 351-359 (2005)
- [17]. Krasilnikov A. et al., “Fundamental Ion Cyclotron Resonance Heating of JET Deuterium Plasmas”, submitted to Plasma Phys. Contr. Fusion.
- [18]. Phillips C.K. et al., Phys. Plasmas **2**, 2427-2434 (1995)
- [19]. Lerche E.A. “Modelling of D majority ICRH at JET: Impact of absorption at the Dopplershifted resonance”, submitted to Plasma Phys. Contr. Fusion
- [20]. Adams J.M. et al, Nucl. Instr. Meth. Phys. Res. **A329**, 277-290 (1993)
- [21]. Korotkov A.A. , et al., Nucl. Fusion **37**, 35-51 (1997)
- [22]. Hjalmarsson A. et al., Rev. Sci. Inst **74**, 1750-1752 (2003)
- [23]. Kallne J. et al., “Advanced Neutron diagnostics for ITER Fusion Experiments”, Report EFDA-JET-CP(04)07-19 (2004)
- [24]. Lerche E.A. et al., Plasma Phys. Control. Fusion **50** 035003 (2008)
- [25]. von Hellermann M.G., Rev. Sci. Instrum. **61**, 3479-3486 (1990)
- [26]. Okano K. et al., Plasma Phys. Control. Fusion **27**, 1069-1076 (1985)
- [27]. M. Messiaen A. et al., Plasma Phys. Control. Fusion **35**, A15-A34 (1993)
- [28]. Choi M. et al., 15th Topical Conference on Radio Frequency Power in Plasmas, Moran, AIP Conf. Proc. **694**, 86-89 (2003)
- [29]. Mantsinen M. , Nuclear Fusion **44**, 33-46 (2004)
- [30]. Van Eester D. et al., “Recent experimental results and modeling of JET (3He)-D scenarios relying on RF heating”, submitted to Plasma Phys. Contr. Fusion.
- [31]. Gorini G. et al., Proc. 31st EPS Conf. on Plasma Physics, London, UK, ECA, Vol. 28GP1.156 (2004)
- [32]. Ruskov E., et al., Phys.Rev.Lett. **82**, 924-927 (1999)
- [33]. Goldston R., et al., J. Comput. Phys. **43**, 61-78 (1981)

D_{an} Pulse No: 61430	Case (a) 0	Case (a) $5m^2/s$	Case (b) 1ms life time for trapped fast ions with $E>30keV$ and $V_{\perp}/V>0.75$ in equatorial midplane on LFS and (neo)classical behaviour for the rest of the fast ions	Case (c) 1ms life time for passing fast ions with $E>30keV$ and $V_{\parallel}/V>0.7$ in equatorial midplane on LFS and (neo)classical behaviour for the rest of the fast ions
Reduction in T power	35%	27%	13%	14%
min (χ^2)	2.76	5.31	5.70	2.37

Table 1: Different cases considered in modelling anomalous fast particle behaviour

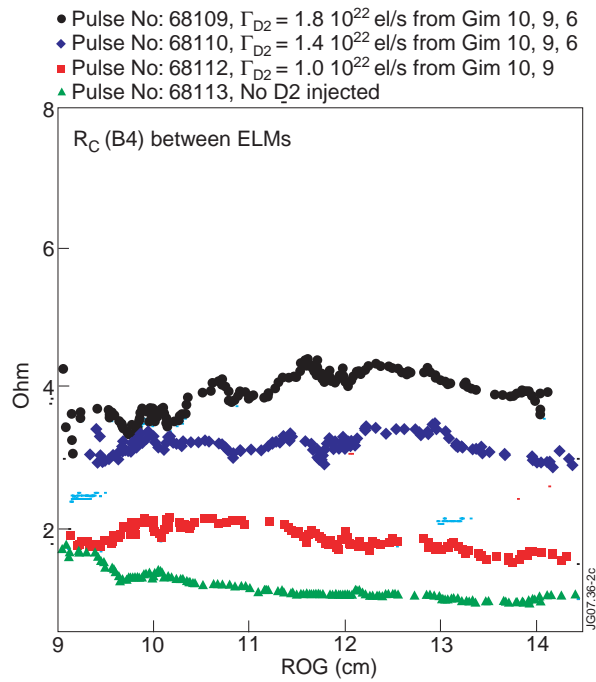


Figure 1: Evolution of the coupling resistance of the B4 antenna strap as a function of ROG and for different levels of D_2 gas injected (using various combinations of GIMs)

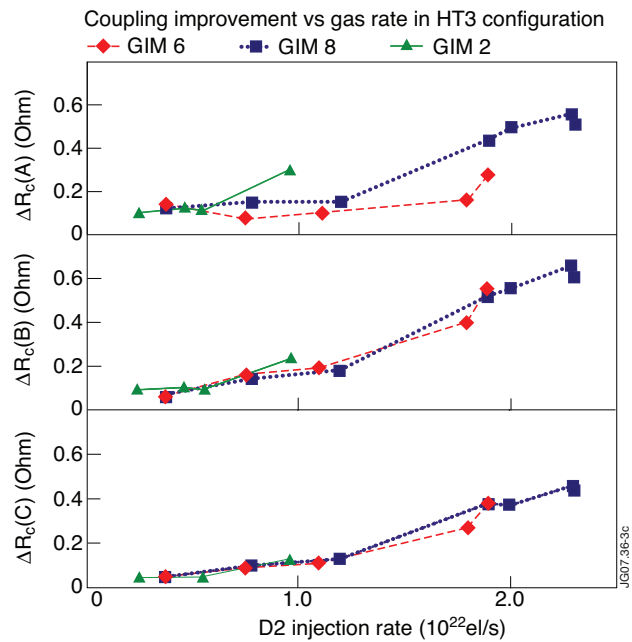


Figure 2: Effect of D_2 gas injection from GIM 6 and GIM 8 on the baseline coupling (i.e. coupling between ELMs) of JET A2 antennas A, B and C.

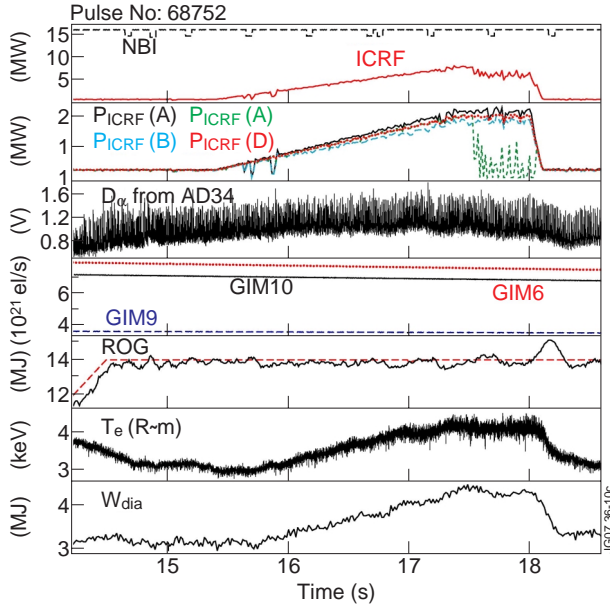


Figure 3: Example of a JET in ELMy H-mode with up to 8MW coupled ICRF power at a ROG of 14 cm and D2 gas injected from GIM 6, 9 and 10.

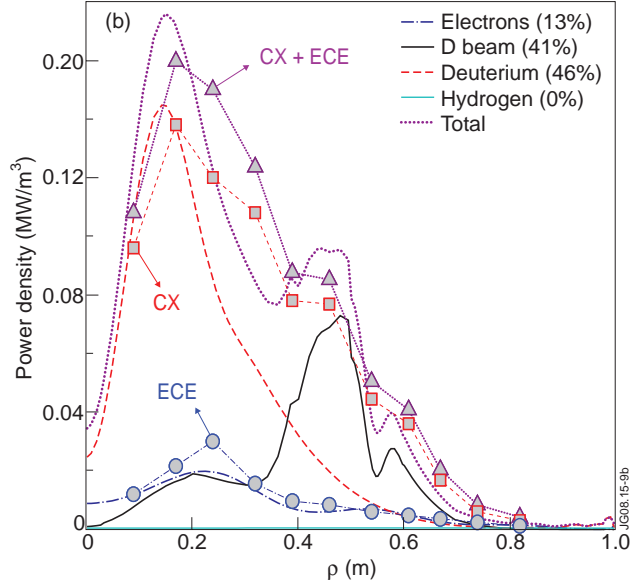


Figure 4: Power absorption profiles obtained with the full-wave CYRANO code for the fundamental D heating scenario in JET using the particle distributions computed from the quasilinear Fokker-Planck code BATCH to represent the NBI deuterons. The experimental power deposition profiles for the electrons and the bulk ions obtained by 'break-in-slope' analysis of the ECE (\bullet) and CX (\blacksquare) signals in Pulse No: 68733 are also included.

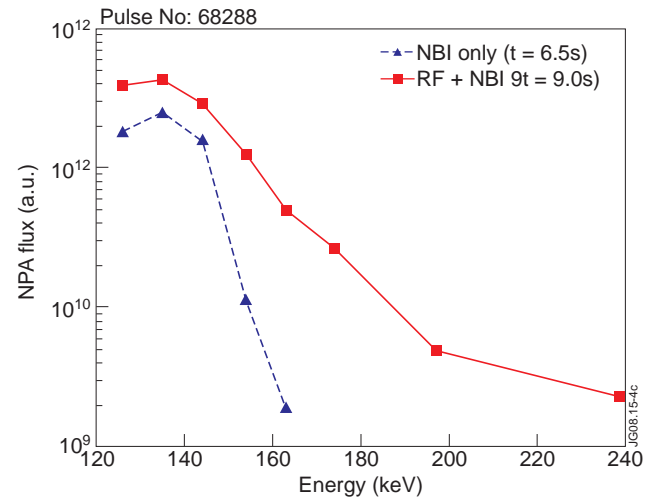
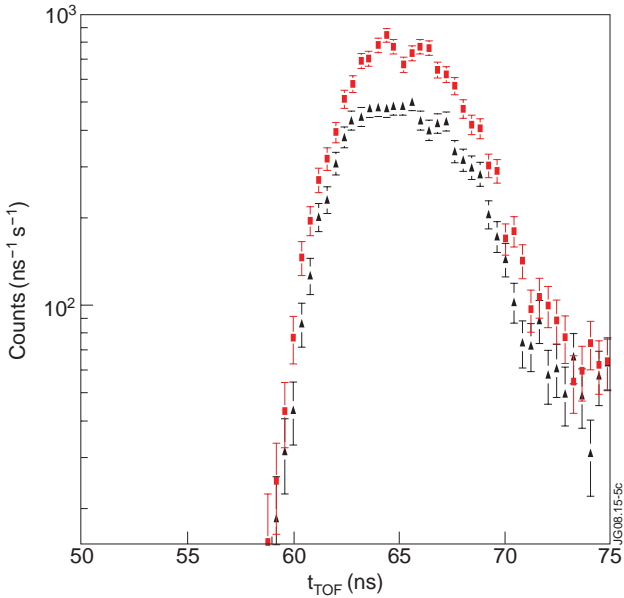


Figure 5: (a) Neutron counts from D-D reactions (~ 2.5 MeV) as function of time-of-flight measured with the neutron spectrometer TOFOR in two phases of Pulse No: 68288: (\blacktriangle) NBI only and (\blacksquare) combined ICRF+NBI; (b) Neutral particle fluxes (in a.u.) measured by the horizontal NPA system (KR2) as function of the fast D energy in two phases of Pulse No: 68288: (\blacktriangle) NBI only and (\blacksquare) combined ICRF + NBI.

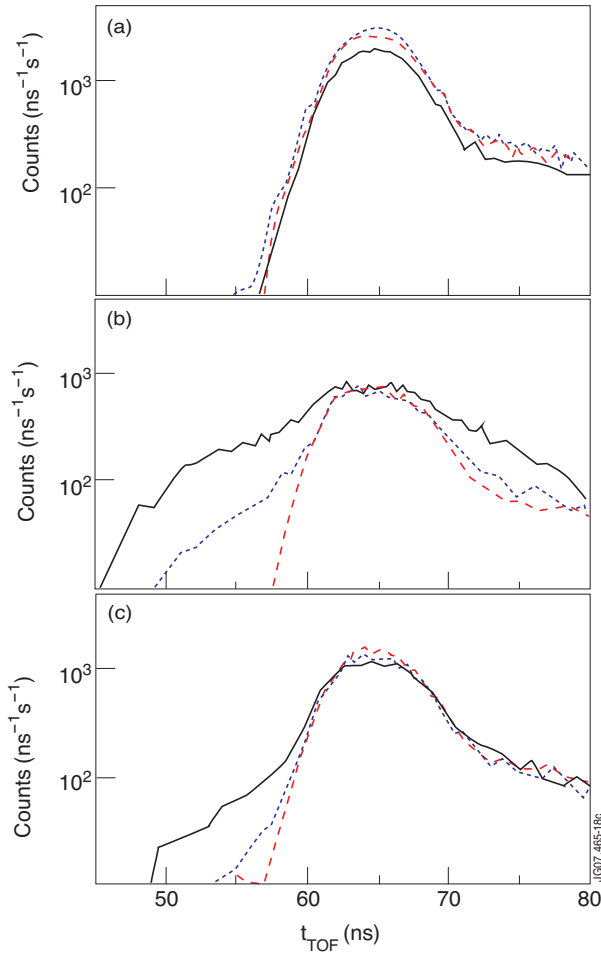


Figure 6: Neutron time of flight spectra (number of counts as function of flight-time) from the TOFOR neutron spectrometer. Data are shown for JET Pulse No's: (a) 69388, (b) 69392 and (c) 69393. For each pulse spectra are shown for three different subsequent time slices during the magnetic field flat top RF+NBI phase: short dashes for $t = 5-6s$, long dashes for $t = 6-7s$, solid lines for $t = 7-8s$.

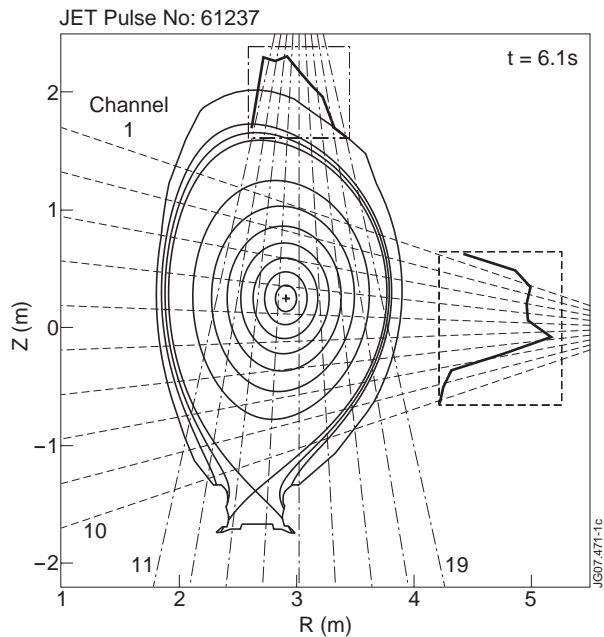


Figure 7: Lines of sight of the neutron camera on JET with channel numbers and a typical profile shape for off-axis NBI heating.

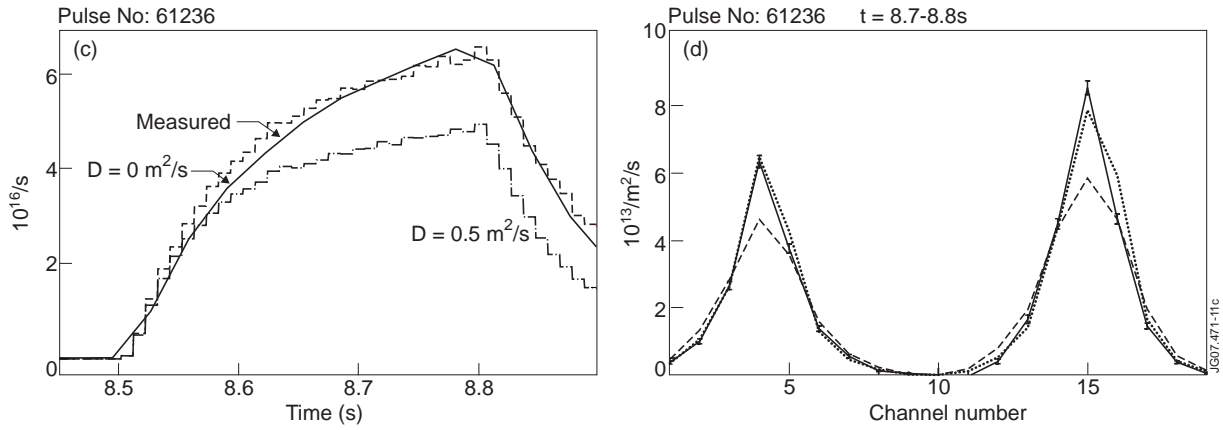


Figure 8: 14MeV neutron rate plot (left) comparing measured and calculated with $D_{an} = 0$ (dotted) and $D_{an} = 0.5 \text{ m}^2/\text{s}$ (dashed) for Pulse No: 61236 (on-axis T) and 14MeV profile (right) comparing measured (solid) with $D_{an} = 0$ (dotted) and $D_{an} = 0.5 \text{ m}^2/\text{s}$ (dashed) simulation). The profiles are integrated over 100ms, the error bars are from a single profile (integrated over 10ms).

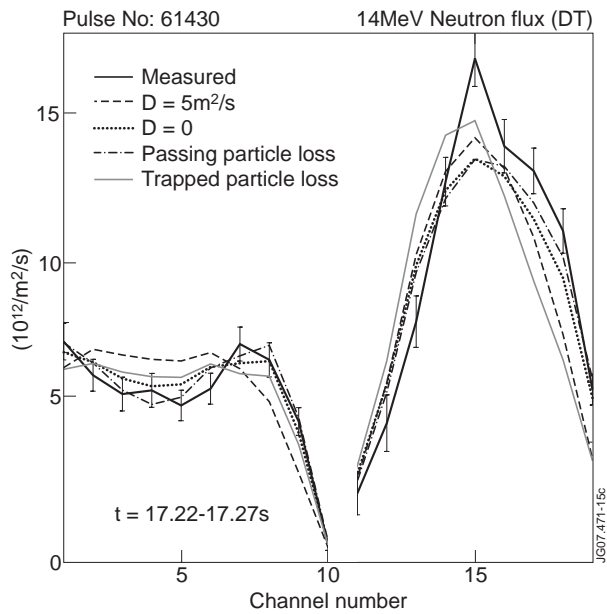


Figure 9: Profiles of 14MeV neutron emission with different forms of anomalous fast ion losses Pulse No: 61430.